Interhemispheric synchronization between the AO and the AAO

Y. Tachibana[1], Y. Inoue[1], K. K. Komatsu[1], T. Nakamura[2], M. Honda[3], K. Ogata[1,4], and K. Yamazaki[1,2]

[1]Faculty of Bioresources, Mie University, Tsu, Japan.

[2]Hokkaido University, Sapporo, Japan

[3]Niigata University, Niigata, Japan

[4]Japan Meteorological Agency, Tsukuba, Japan

2nd version, Submitted date: 7 November, Paper #2018GL079921

Key Points:

- In-phase synchronicity between the Arctic and Antarctic Oscillations was found in February and October.
- Tropical ocean variations such as El Niño–Southern Oscillation seem to be of little or no importance to this synchronicity.
- The stratospheric meridional circulation may be a key factor leading to synchronization.

Abstract

Teleconnections between lower and higher latitude regions are widely known in both the Northern and Southern Hemispheres. To broaden our view of these teleconnections, we searched a reanalysis dataset for evidence of a teleconnection between the Arctic Oscillation (AO) and the Antarctic Oscillation (AAO), two widely separated circumpolar phenomena. Statistical analysis of the Japanese 55-year reanalysis dataset showed significant in-phase synchronization between the AO and AAO, particularly in October and February, with a vertical structure extending from the troposphere to the stratosphere. This vertical structure may suggest a stratospheric control, and we did not find a significant signature indicating a tropical ocean control. We also observed decadal-scale modulation of the synchronicity. Observational evidence implies that the stratospheric meridional circulation may be responsible for AO–AAO synchronization.

Plain Language summary

The Arctic Oscillation (AO) and the Antarctic Oscillation (AAO) are dominant atmospheric variability patterns in the Northern and Southern hemispheres, respectively. Each is a pressure seesaw between the pole and the midlatitudes that remotely affects weather, climate, and environment around the world. We showed interhemispheric in-phase synchronization between the AO and AAO in October and February, and we also found decadal-scale variation of the synchronicity. Because the vertical structure of the AO–AAO synchronization extends from the troposphere to the stratosphere, stratospheric variations may be responsible for the synchronization. This finding of AO–AAO synchronization points the way to a better understanding of past, present, and future pole-to-pole climatic relationships and improvements in long-term weather forecasts.

1 Introduction

The Arctic Oscillation (AO) is the leading mode of large-scale atmospheric variations in middle to high latitudes of the Northern Hemisphere (Thompson and Wallace, 1998), and its impact on extreme weather events in the Northern Hemisphere is significantly large in all seasons (e.g., Thompson and Wallace, 2001). The Antarctic Oscillation (AAO) is the leading mode of atmospheric variations in the middle to high latitudes of the Southern Hemisphere (Gong and Wang, 1999; Mo, 2000), and it is known to have two-way interaction with the evolution of the ozone hole (Thompson and Solomon, 2002). The AO and AAO are thus both scientifically and socio-economically important. In accordance with established convention, the positive phase of the AO or AAO indicates that sea level pressure is lower than normal in both circumpolar regions and higher than normal in both midlatitude regions, and the negative phase indicates the reverse signature. Many studies have investigated the causes of long-term variations of both the AO and the AAO. For example, the recent shift toward a more negative phase of the AO was influenced by the Arctic sea ice reduction (e.g., Nakamura et al., 2015a), and the AAO is influenced by stratospheric circulation trends associated with anthropogenic ozone forcing (Thompson and Solomon, 2002; Thompson et al., 2011). In general, however, causes of variations in the AO and AAO have been studied independently. Because the AO and AAO are widely separated circumpolar phenomena, interactions or teleconnections between them have been largely disregarded. Guan and Yamagata (2001), Lu at al. (2008) and Guan et al. (2010) described the interhemispheric connection as a seesaw-like oscillation of mean hemispheric surface air pressures between the Northern and Southern Hemispheres. Tang and Guan (2015) described a polar-tropical seesaw mode, but to the best of our knowledge no one has examined synchronicity between the AO and AAO.

A possible driver of synchronization of mid- and high-latitude variations of the AO and AAO between the two hemispheres is the variation of tropical sea surface temperature (SST). For example, remote impacts of El Niño-Southern Oscillation (ENSO) have been observed on the weather at high latitudes in both hemispheres through the Pacific–North American (e.g., Trenberth et al., 1998) and the Pacific–South American (e.g., Karoly, 1989) teleconnection patterns. Tropical convective activity associated with the Madden–Julian Oscillation also affects the weather at high latitudes (Zhou and Miller, 2005; Nauman and Vargas, 2010). Modification of planetary-scale wave pathways by the stratospheric quasi-biennial oscillation (QBO) might also affect polar vortex intensity and the resultant sea level pressure anomalies over high-latitude regions (Holton–Tan effect; Holton and Tan, 1980; O'Sullivan and Young, 1992; Marshall and Scaife, 2009).

Conversely, remote influences of high-latitude atmospheric variations on the tropics have also been reported. For example, the changes in midlatitude circulation that accompany the AO can affect tropical convective activity and trigger an El Niño event (e.g., Nakamura et al., 2006; 2007; Oshika et al., 2014; Chen et al., 2017). Moreover, intensification of the stratospheric meridional circulation (i.e., the Brewer–Dobson circulation) intensifies rapid tropical convective cloud formation during sudden stratospheric warming (SSW) events in both the Southern (Eguchi and Kodera, 2007) and Northern (Kodera et al., 2011) hemispheres. SSW events in the Northern (Southern) Hemisphere often accompany the negative phase of the AO (AAO) (e.g., Baldwin and Dunkerton, 2001; Gerber et al., 2010). The enhancement of tropical convective activity by extratropical forcing from one hemisphere might influence in turn the extratropical atmosphere of the opposite hemisphere, because the large latent heat release associated with tropical convective clouds is widely recognized as a source of tropical influence on the high-latitude atmosphere.

From these lines of evidence suggesting a remote connection between the tropics and high-latitude regions of both hemispheres, it is reasonable to infer that a physically based AO–AAO synchronicity might also exist. The next step, therefore, is to examine this inference by looking for synchronicity between the AAO and AO.

The principal purpose of the present study is to detect this inferred synchronization in a reanalysis dataset. Then we examined the seasonal dependency and decadal-scale modulation of the detected synchronicity as well as the interhemispheric-scale meridional–vertical structures associated with AO-AAO synchronization. Clarifying the mechanism of the synchronization is beyond our scope, but we make a discussion on a possible physical process.

2 Data and Methods

We used the Japanese 55-year Reanalysis (JRA-55) product for 1979–2016 (Kobayashi et al., 2015). Following Gong and Wang (1999), we defined AO and AAO indices simply as the normalized monthly mean difference in zonal mean sea level pressure (SLP) between the latitudes of 65° and 40° in each respective hemisphere (i.e., SLP at 40°S or N minus SLP at 65°S or N, where a positive (negative) index value indicates a low (high) SLP anomaly in the polar region). The AO index defined by Gong and Wang (1999), which the present paper used, is almost identical to an original index by an EOF analysis defined by Thompson and Wallace (1998) in winter. Correlation coefficients between the two indices are over 0.7 in winter. The EOF analysis tends to capture characteristics of the winter patterns because of their largest variability during winter. Present study compares between opposite season in the Northern and

Southern Hemispheres, i.e., between winter and summer, or between spring and autumn. We thus use the simple index defined by Gong and Wang (1999). We used linear regression and correlation analyses of the data to identify synchronicity between the AO and AAO. We also calculated running correlation coefficients within a 25-year window to examine decadal-scale modulation of the synchronicity. We confirmed that the decadal modulation did not depend on the length of the window. An AO+AAO index is additionally used. The definition of the AO+AAO index is the sum of the normalized AO index and the normalized AAO index. Large absolute value of the index tends to be large when both the AO and AAO are synchronized.

Singular value decomposition (SVD) analysis, which statistically isolate significant connection between two pieces of multivariate variations, is widely used for seeking large-scale atmosphere-ocean connection (e.g., Wallace et al., 1992; Nakamura et al., 2015b). Present study applies SVD analysis to detect covariant meridional–vertical structures involving the troposphere and stratosphere. Because SVD needs to prepare two field variables, we applied to monthly mean anomaly fields of zonal mean geopotential height poleward of 40° at altitudes between 1000 and 10 hPa in the Southern and Northern hemispheres.

3. Evidence of AO–AAO Synchronicity in the JRA-55 dataset

We first calculated correlation coefficients between the monthly mean AO and AAO indices (Figure 1, right column). The correlation coefficients for February and October during the entire study period (1979–2016), 0.41 and 0.36, respectively, were statistically significant at the 95% level (*t*-test). Moreover, the 25-year running correlations (Figure 1, color gradations) show that during some sub-periods, the correlation coefficients in February and October exceeded 0.5. We further executed 19-, 21-, and 23-year running correlation analyses, and overall correlation patterns as shown in Figure 1 are also seen. Here, positive correlations indicate that SLP was lower than normal in both circumpolar regions and higher than normal in both midlatitude regions, and negative correlations indicate the reverse. Thus, in these two months, the polarities of the AO and AAO tended to be in phase. The interannual time series of AO–AAO synchronicity in February and October (Figure 2) clearly shows in-phase synchronization between the AO and AAO, especially during the sub-period when the correlation coefficient was highest. High correlation sub-periods were between 1980s and the beginning of 2000s. Notably, this coherent variation occurs on an interannual timescale and is not due to a long-term trend. In February, the correlation was mostly positive during the study period, and the maximum correlation of 0.51 was observed during 1980–2004. In October, the maximum correlation of 0.56 was observed during 1981–2005. These maximum correlations were statistically significant at the 99% confidence level.

We next examined connectivity between the Northern Hemisphere and the Southern Hemisphere by applying SVD analysis to the 25-year periods with the maximum correlation between the indices. The monthly mean homogeneous regression map of the first SVD mode (SVD1) for the Southern Hemisphere in February showed a strong AO signature in the Northern Hemisphere: that is, strongly negative values in Arctic latitudes and strongly positive values in midlatitude regions (Figure 3, top left). In the map for the Northern Hemisphere, we observed an AAO signature, that is, negative values over the Antarctic region and positive values in the midlatitudes of the Southern Hemisphere (top center). Because SVD1 shows the largest covariant pattern between two fields, the appearance of AO and AAO signals in both homogenous maps signifies AO–AAO synchronicity. In other words, geostrophic westerlies that are stronger (weaker) than normal tend to blow synchronously in both hemispheres. Furthermore, the AO and AAO signals are not confined to the troposphere but extend into the stratosphere; therefore, as is often observed during SSW events, stratospheric variation may influence the troposphere. The interannual variation of the normalized expansion coefficients for the Northern and Southern Hemispheres in February (Figure 3, upper right) are clearly synchronized with each other, and SVD1 explained 53.0% of the squared covariance fraction (SCF). Correlation coefficient of the expansion coefficients for the Nouthern Hemisphere (green curves of Figure 3) with the AO index (red curves of Figure 2) are 0.61 and 0.76 in February and October respectively.

SVD1 also showed in-phase synchronicity, with the structure extending into the stratosphere, between the AO and AAO in October (Figure 3, lower panels). The interannual variations of the expansion coefficients for the Northern and Southern hemispheres were also significantly correlated in October, although the correlation was weaker than the correlation of the SLP-based indices. SVD1 explained 52.4% of the SCF. Correlation coefficient of the expansion coefficients for the Southern Hemisphere (black curves of Figure 3) with the AAO index (red curves of Figure 2) are 0.90 and 0.93 in February and October respectively.

Interestingly, in both February and October, the SVD1 pattern exhibited an asymmetric vertical structure. In February the activity center of the AO signal is in the stratosphere and that of the AAO is in the lower stratosphere to upper troposphere (Figure 3, upper panels). Conversely, in October the activity center of the AAO signal is in the stratosphere and that of the AO is in the lower stratosphere to upper troposphere (Figure 3, lower panels). Thus, the dominant signal of the winter hemisphere is in the stratosphere, whereas that of the summer hemisphere is in the troposphere. Because SSW events occur more often in February and October in the Northern and Southern Hemispheres, respectively, than in the other months, this asymmetric structure may indicate that the remote connection between the Northern and Southern hemispheres originates from stratospheric variations such as SSW events that occur during the active season.

We next show zonal mean regression fields on the meridional vertical plain with AO and AAO indices in February and October in order to confirm the pattern extracted by SVD can be reproduced by these simple regression analyses. When we examined zonal-mean regression fields of zonal-mean geopotential height against the AO and AAO indices in February on the meridional–vertical plane (Figure 4, upper panels), we observed two positive and negative anomaly pairs, that is, the AAO and AO signatures, in the troposphere of both hemispheres. In October, on the regression map against the AAO index (Figure 4, lower left), we observed a clear AAO signature in the troposphere of the Southern Hemisphere that extended into the stratosphere. Further, the positive anomaly in the Southern Hemisphere extended into the lower stratosphere in the equatorial region and then descended into the troposphere of the Northern Hemisphere; thus, it formed an arch-like structure over the equatorial troposphere. A positive and negative anomaly pair, that is, the AO signature, was also seen in the troposphere of the Northern Hemisphere in October (Figure 4, lower left). On the regression map against the AO index, negative anomalies were seen in the circumpolar region in the Southern Hemisphere (Figure 4, lower right).

4. Possible Causes of Synchronicity between the AO and AAO

The principal aim of this study was to establish that synchronicity existed between the AO and the AAO. Although clarifying the mechanism is beyond our scope, we also considered possible mechanisms of synchronicity. Our statistical analyses showed that variations of the AO and AAO were in phase during February and October. The correlation coefficients between seasonal mean AO and AAO indices were weaker than those of monthly mean indices. This seasonal dependence might be key to understanding the mechanism of AO–AAO synchronicity.

The potential of tropical oceanic variations such as ENSO to affect the atmosphere over both poles simultaneously is large. It is natural, however, to consider that forcing by a long-lasting event such as ENSO would be more persistent than forcing by a short-term event. If the dominant influence on AO–AAO synchronicity was of tropical origin, then the synchronicity should continue for a few months or longer. Contrary to this expectation, correlations between the AO and AAO indices were more highly positive when monthly mean values were compared than when 3-month means were compared. In fact, when we regressed the sea surface temperature (SST) anomaly against the AO+AAO index, which has a large absolute value when they are synchronized, we found no significant signature in the tropics in February, and only a very weak La Niña-like signature in October (Figure S1). Furthermore, an atmospheric general circulation model (AGCM) simulation that did not take account of interannual variations of global SST could partly represent the AO–AAO synchronicity in October (Figure S2). These results suggest that tropical oceanic SST variation is of little importance, at least with regard to the in-phase synchronicity of the AO and AAO. By the same logic, the QBO, because its period is much longer than a month, is unlikely to be a cause of the synchronicity. In fact, regression of the zonal-mean zonal wind field against the AO+AAO index also showed no significant anomalies in the tropical stratosphere (Figure S3).

Dynamical variations in the polar region have been shown to affect tropical convective activity; for example, atmospheric convective activity in the tropical region may be controlled via changes in the stratospheric meridional circulation associated with SSWs (Eguchi and

Kodera, 2007; Kodera et al., 2011) or via tropospheric eddy dynamics associated with the AO (Oshika et al., 2014; Chen et al., 2017). Because the large latent heat release that accompanies tropical convective clouds is widely recognized as the mechanism of a tropical influence on the high-latitude atmosphere, tropical convective cloud activity that has been influenced by extratropical dynamical variations might mediate the propagation of extratropical signatures from one pole to the opposite pole. These considerations suggest that a sporadic extratropical event might be responsible for the AO–AAO synchronization that we detected. A SSW event is a likely candidate for this sporadic event. The vertical structure of the anomalous geopotential height pattern of AO–AAO synchronicity is asymmetric between the two hemispheres: in February, signals are stronger in the stratosphere of the Northern Hemisphere, and in October, they are stronger in the stratosphere of the Southern Hemisphere, in each case compared with the signal strength in the opposite hemisphere (Figure 3). The signals extending to the stratosphere, the so-called Northern Hemisphere annular mode/Southern Hemisphere annular mode (NAM/SAM) pattern, are closely related to SSW occurrences. SSW events often accompany the negative phase of the AO (Baldwin and Dunkerton, 2001). An SSW that is accompanied by intensification of stratospheric meridional circulation (i.e., Brewer–Dobson circulation) remotely controls tropical convective cloud activity (Eguchi and Kodera, 2007; Kodera et al., 2011). This SSW-controlled tropical cloud activity might further influence the extratropical atmosphere in the opposite hemisphere.

We note again that the seasonality of the AO-AAO synchronicity has an important implication. Climatologically, February is the month with the most SSW event activity in the Northern Hemisphere (e.g., Hu et al., 2014). Surface anomalies due to downward influences of SSW events also appear in February. The frequent occurrence of SSW events in February might account for the large correlation between the AO and AAO in that month. Similarly, the largest variability in polar vortex intensity in the Southern Hemisphere is observed in October. The year 2002 is illustrative. A SSW event was observed in the Southern Hemisphere in 2002 (e.g., Eguchi and Kodera 2007), and the negative phases of the AO and AAO were also strongly synchronized in that year (Figure 2). In late autumn and early winter in 2002, it was extremely cold over the mid-latitude Northern Hemisphere, in particular over Europe and East Asia. Besides, Arctic sea ice in late autumn and following winter was higher than normal, and the high ice condition was associated with negative phase of AO (Ogi and Wallace, 2007). These lines of inference lead us to consider that the AAO and AO may be linked via the stratosphere. The AO-AAO connections in the February and October do not look symmetric in the seasonal march. From February to October, we have 8 months whereas from October to February we have 4 months. Interestingly, the variance of the stratospheric polar night jet in individual hemispheres are not symmetric: the peak period in the Northern hemisphere is in January or February which corresponds to the occurrence of SSW, while in the Southern Hemisphere, the peak is in October or November (Figure S4). Therefore, the stratosphere-troposphere connection may tend to appear in these months, in which AO-AAO synchronization appears. QBO could be another major candidate of a cause of the inter-hemispheric synchronization, because of its correlation to the stratospheric polar vortex variations well known as Holton-Tan effect (Holton and Tan, 1980). However, considering very low stratospheric variations in the summer hemisphere (Figure S4), there is difficulty to apply the QBO-polar vortex relationship to the inter-hemispheric synchronicity in the troposphere. In the next step, it should be considered that how the stratospheric signature propagates the tropospheric summer hemisphere. It is known that interhemispheric connection exists in the mesosphere (e.g., Kornich and Becker, 2010), in which the winter hemisphere has an influence on the summer hemisphere. This interhemispheric mesospheric process might be another intermediator for the AO-AAO synchronization in the troposphere and stratosphere. However, we consider that downward influence in the summer hemisphere unlikely occurs because the variance of the summer stratosphere is small (Figure S4).

5. Summary

This study confirmed the existence of in-phase synchronization between the AAO and AO indices in February and October on an interannual time scale. In both hemispheres, lows are tend to be in circumpolar regions simultaneously, whereas the highs tend to be in the midlatitude regions and vice versa. In other words, stronger than normal geostrophic westerlies tend to blow synchronously in both hemispheres, or weaker than normal geostrophic westerlies tend to blow in both hemispheres. Therefore, air masses in the circumpolar regions of both hemispheres move simultaneously and in phase from higher to lower latitudes, or from lower to higher latitudes. The synchronization in other months, however, is much weaker.

In this study, we did not try to definitively identify the mechanism of the synchronization, but we offer the following considerations. Tropical oceanic variations such as ENSO are apparently of little importance to the AO–AAO synchronicity, although tropical variations are known to be a driver of high-latitude phenomena. However, stratospheric dynamics related to SSW events may provide a bridge across the tropics between high-latitude regions of the two hemispheres. In addition, the results of an AGCM simulation, albeit one that was not specifically related to this study, support the observational evidence that tropical variations are not important

(See Supporting Information). In the future, a modeling study with a focus on the stratospheric role in AO–AAO synchronicity should be conducted.

Figure Captions

Figure 1. Correlations between the AO and AAO indices. The column on the right shows the correlation coefficients between monthly mean AO and AAO indices for each month during the whole study period (1979–2016). The correlation coefficients shown in bold are statistically significant at the 95% level (*t*-test). The color scale shows 25-year running correlation coefficients between the AO and AAO indices. The years shown on the horizontal axis indicate the center of each 25-year window in which the correlation was calculated. The stars indicate the 25-year period with the highest correlation coefficients for February (0.51) and October (0.56).

Figure 2. Interannual AO–AAO synchronicity. Monthly mean values of the AAO and AO indices in February (top) and October (bottom). The vertical axis shows the normalized values of the indices divided by the individual standard deviations. The thick lines indicate the 25-year sub-period in each month with the highest correlation coefficient (indicated by the star symbol in Figure 1).

Figure 3. Zonal-mean geopotential height pattern and year-to-year variations, derived from the first SVD mode. SVD was applied to zonal-mean monthly mean geopotential heights in February (upper panels) and October (lower panels). (left column) Homogeneous regression maps for the Southern Hemisphere. Horizontal and vertical axes are latitude and altitude, respectively. (center column) Homogeneous regression maps for the Northern Hemisphere. In each month, areas within the green boxes in the Southern and Northern hemispheres were paired for the SVD

calculation. The contour/color shading interval is 10 m, and red and blue colors indicate positive and negative values, respectively. (right) Time series of the normalized expansion coefficients divided by the standard deviation for the Southern Hemisphere (black curve) and the Northern Hemisphere (green curve). The squared covariance fraction (SCF) and correlation coefficient are shown in the upper left and upper right corners, respectively.

Figure 4. Meridional–vertical patterns of zonal-mean geopotential height regressed against the (left panels) AAO and (right panels) AO indices. Horizontal and vertical axes show latitude and altitude, respectively. The upper and lower panels show results for February and October, respectively. The contour interval is 10 m, and color shading indicates the level of statistical significance. Red and yellow shades indicate positive correlations, and blue shades indicate negative correlations.

Acknowledgments and Data

The authors acknowledge K. Kodera for encouraging us to develop our idea. Comments from anonymous reviewers were also helpful. This study was partly supported by the Ministry of Education, Culture, Sports, Science and Technology through a Grant-in-Aid for Scientific Research on Innovative Areas (Grant Number 16K13880 and 17H02958) and by the Arctic Challenge for Sustainability Project and Belmont Forum InterDec Project. All figures were compiled by using GrADS and Generic Mapping Tools software. The analyzed datasets along with the initial and boundary conditions of the numerical experiments are available to the public as indicated in the Methods section and the Supporting Information. The authors declare no

competing financial interests in relation to the work described. The authors declare no competing non-financial interests as well.

References

Baldwin, M. P., and T. J. Dunkerton (2001), Stratospheric harbingers of anomalous weather regimes, *Science*, **294**, 581–584.

Chen, S., W. Chen, and B. Yu (2017), The influence of boreal spring Arctic Oscillation on the subsequent winter ENSO in CMIP5 models, *Clim. Dyn.*, **48**, 2949–2965. https://doi.org/10.1007/s00382-016-3243-z.

Eguchi, N. and K. Kodera (2007), Impact of the 2002, southern hemisphere, stratospheric warming on the tropical cirrus clouds and convective activity, *Geophys. Res. Lett.*, **34**, L05819, doi:10.1029/2006GL028744.

Gerber, E. P., et al. (2010), Stratosphere - troposphere coupling and annular mode variability in chemistry - climate models, *J. Geophys. Res.*, **115**, D00M06, doi:10.1029/2009JD013770.

Gong, D. and S. Wang (1999), Definition of Antarctic Oscillation index, *Geophys. Res. Lett.*, **26**, 459–462, doi:10.1029/1999GL900003.

Guan, Z., and T. Yamagata (2001), Interhemispheric Oscillations in the Surface Air Pressure Field, *Geophys. Res. Lett.*, **28**, 263–266.

Guan, Z., C. H. Lu, S. L. Mei, and J. Cong (2010), Seasonality of interannual inter-hemispheric oscillations over the past five decades, *Adv. Atmos. Sci.*, **27**, 1043-1050, doi: 10.1007 /s00376-009-9126-z.

Holton, J. R., and H.-C. Tan (1980), The influence of the equatorial quasi-biennial oscillation on the global circulation at 50mb, *J. Atmos. Sci.*, **37**, 2200–2208

Hu, J. G., R. Ren, and H. Xu (2014), Occurrence of winter stratospheric sudden warming events and the seasonal timing of spring stratospheric final warming, *J. Atmos. Sci.*, **71**, 2319–2334, doi:10.1175/JAS-D-13-0349.1.

Karoly, D. J. (1989), Southern Hemisphere circulation features associated with El Niño – Southern Oscillation events, *J. Clim.*, **2**, 1239–1252,

Kobayashi, S., Y. Ota, Y. Harada, A. Ebita, M. Moriya, H. Onoda, K. Onogi, H. Kamahori, C. Kobayashi, H. Endo, K. Miyaoka, and K. Takahashi (2015), The JRA-55 Reanalysis: General specifications and basic characteristics, *J. Meteor. Soc. Japan*, **93**, 5–48, doi:10.2151/jmsj.2015-001.

Kodera, K., N. Eguchi, J. N. Lee, Y. Kuroda, and S. Yukimoto (2011), Sudden chgange in the tropical straospheric and tropopshperic Circulation during January 2009, *J. Meteor. Soc. Japan*, **89**, 283–290, doi:10.2151/jmsj.2011-308.

Kornich, H. and E. Becker (2010), A simple model for the interhemispheric coupling of the middle atmosphere circulation. *Adv. Space Research*, **45**, 661-668, DOI: 10.1016/j.asr.2009.11.001

Lu, C., Z. Guan, S. Mei, and Q. Yujing (2008), The seasonal cycle of interhemispheric oscillations in mass field of the global atmosphere, Chin. Sci. Bull., 53, 3226. https://doi.org/10.1007/s11434-008-0316-3

Marshall, A. G., and A. A. Scaife (2009), Impact of the QBO on surface winter climate, *J. Geophys. Res.*, **114**, D18110, doi:10.1029/2009JD011737.

Mo, K. C. (2000), Relationships between Low-Frequency Variability in the Southern Hemisphere and Sea Surface Temperature Anomalies, *J. Climate*, **13**, 3599-3610.

Nakamura T., Y. Tachibana, M. Honda, and S. Yamane (2006), Influence of the Northern Hemisphere annular mode on ENSO by modulating westerly wind bursts, *Geophys. Res. Lett.*, **33**, L07709, doi: 10.1029/2005GL025432.

Nakamura T., Y. Tachibana, and H. Shimoda (2007), Importance of cold and dry surges in substantiating the NAM and ENSO relationship, *Geophys. Res. Lett.*, **34**, L22703, doi: 10.1029/2007GL031220.

Nakamura, T., K. Yamazaki, K. Iwamoto, M. Honda, Y. Miyoshi, Y. Ogawa, and J. Ukita (2015a), A negative phase shift of the winter AO/NAO due to the recent Arctic sea-ice reduction in late autumn, *J. Geophys. Res. Atmos.*, **120**, 3209–3227. doi:10.1002/2014JD022848

Nakamura T., M. Oshika, M. Hara, and Y. Tachibana, Impact of the winter North Atlantic Oscillation (NAO) on the Western Pacific (WP) pattern in the following winter through Arctic sea ice and ENSO. Part II: Multi-model evaluation of the NAO-ENSO linkage (2015b), *Clim. Dyn.*, **40**, doi: 10.1007/s00382-015-2556-7.

Naumann, G., and W. M. Vargas (2010), Joint diagnostic of the surface air temperature in southern South America and the Madden–Julian oscillation, *Wea. Forecasting*, **25**, 1275–1280.

Ogata K, Y. Tachibana, Y. Udagawa, K. Oshima, and K. Yoshida (2013), Influence of sea ice anomaly in the Pacific sector of the Southern Ocean upon atmospheric curculation uysing AGCM, *Umi to sora*, **89**, 19–23, http://dl.ndl.go.jp/info:ndljp/pid/10116137

Ogi, M., and J. M. Wallace (2007), Summer minimum Arctic sea ice extent and the associated summer atmospheric circulation, Geophys. Res. Lett.,34, L12705, doi:10.1029/2007GL029897.

Oshika M., Y. Tachibana, T. Nakamura (2014), Impact of the winter North Atlantic Oscillation (NAO) on the Western Pacific (WP) pattern in the following winter through Arctic sea ice and ENSO: part I—observational evidence, *Clim. Dyn.*, doi: 10.1007/s00382-014-2384-1

O'Sullivan, D., and R. E. Young (1992), Modeling the quasi-biennial oscillation's effect on the winter stratosphere circulation, *J. Atmos. Sci.*, **49**, 2437–2448.

Tang, W. and Z. Guan (2015), ENSO-independent contemporaneous variations of anomalous circulations in the Northern and Southern Hemispheres: The polar-tropical seesaw mode. *J. Meteor. Res.*, **29**, 917-934, doi: 10.1007/s13351-015-5095-6.

Thompson, D. W. J., and S. Solomon (2002), Interpretation of recent Southern Hemisphere climate change, *Science*, **296**, 895–899, doi:10.1126/science.1069270.

Thompson, D. W. J., and J. M. Wallace (1998), The Arctic Oscillation signature in the wintertime geopotential height and temperature fields, *Geophys. Res. Lett.*, **25**, 1297–1300.

Thompson, D. W. J., and J. M. Wallace (2001), Regional climate impacts of the Northern Hemisphere annular mode, *Science*, **293**, 85–89, doi:10.1126/science.1058958.

Thompson, D. W. J., S. Solomon, P. J. Kushner, M. H. England, K. M. Grise, and D. J. Karoly (2011), Signatures of the Antarctic ozone hole in Southern Hemisphere surface climate change, *Nature Geoscience*, **4**, 741–749, doi:10.1038/NGEO1296.

Trenberth, K. E., G. W. Branstator, D. Karoly, A. Kumar, N.-C. Lau, and C. Ropelewski (1998), Progress during TOGA in understanding and modeling global teleconnections associated with tropical sea surface temperatures, *J. Geophys. Res.*, **103**(C7), 14291–14324, doi:10.1029/97JC01444.

Wallace, J. M., C. Smith, and C. S. Bretherton (1992), Singular value decomposition of wintertime sea surface temperature and 500-mb height anomalies, *J. Climate*, **5**, 561–576.

Zhou, S., and A. J. Miller (2005), The interaction of the Madden–Julian oscillation and the Arctic Oscillation, *J. Climate*, **18**, 143–159.

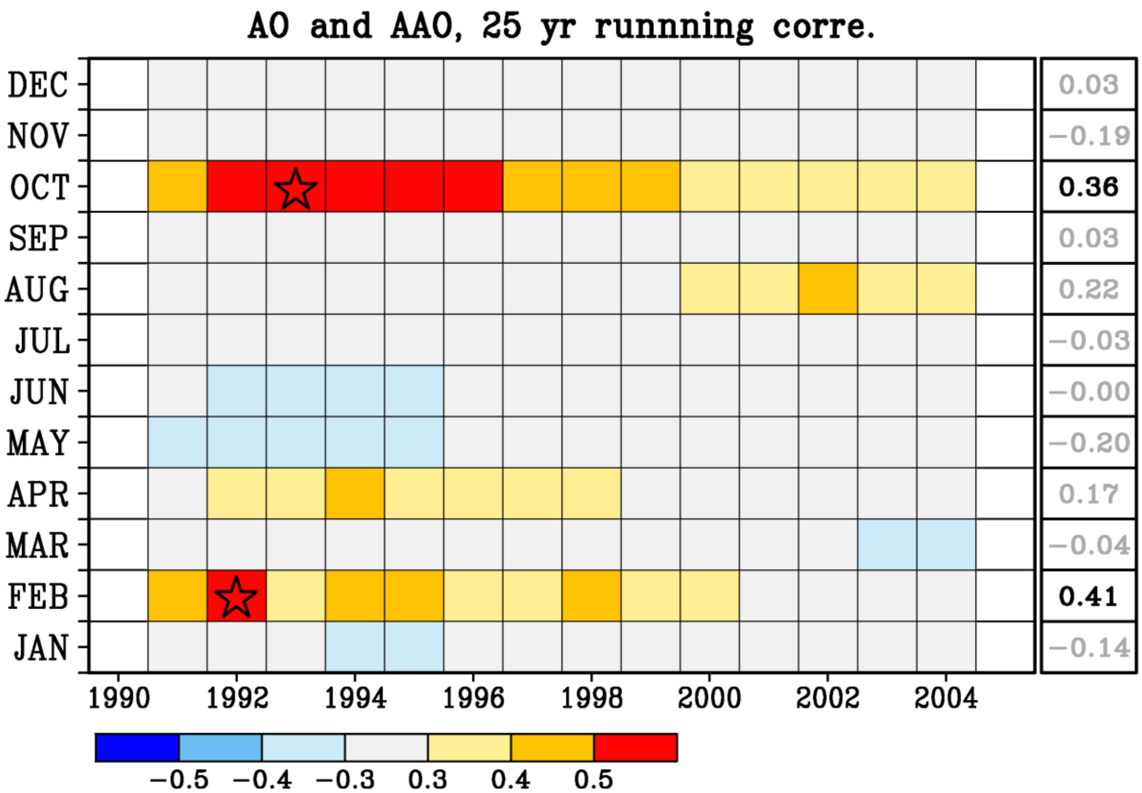

Figure 1. Correlations between the AO and AAO indices. The column on the right shows the correlation coefficients between monthly mean AO and AAO indices for each month during the whole study period (1979–2016). The correlation coefficients shown in bold are statistically significant at the 95% level (*t*-test). The color scale shows 25-year running correlation coefficients between the AO and AAO indices. The years shown on the horizontal axis indicate the center of each 25-year window in which the correlation was calculated. The stars indicate the 25-year period with the highest correlation coefficients for February (0.51) and October (0.56).

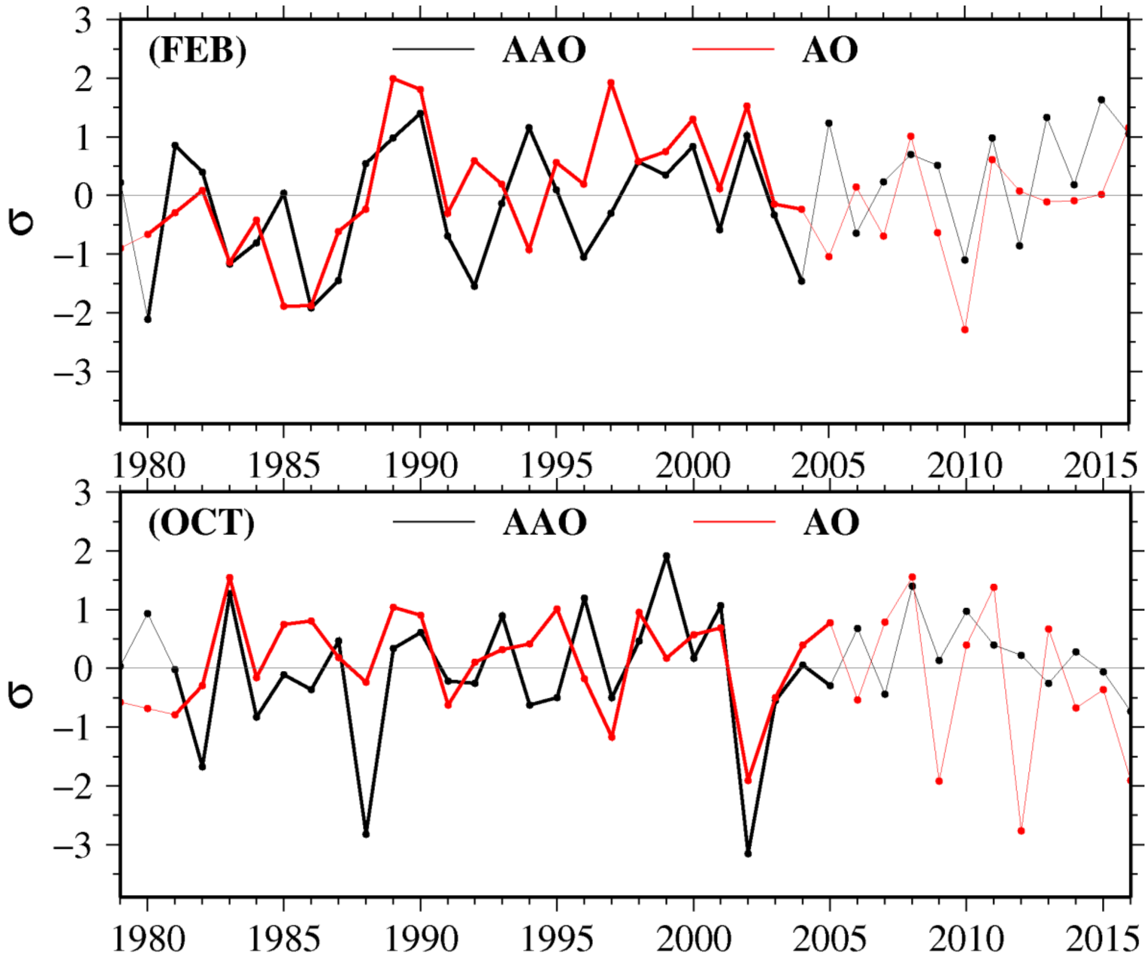

Figure 2. Interannual AO–AAO synchronicity. Monthly mean values of the AAO and AO indices in February (top) and October (bottom). The vertical axis shows the normalized values of the indices divided by the individual standard deviations. The thick lines indicate the 25-year sub-period in each month with the highest correlation coefficient (indicated by the star symbol in Figure 1).

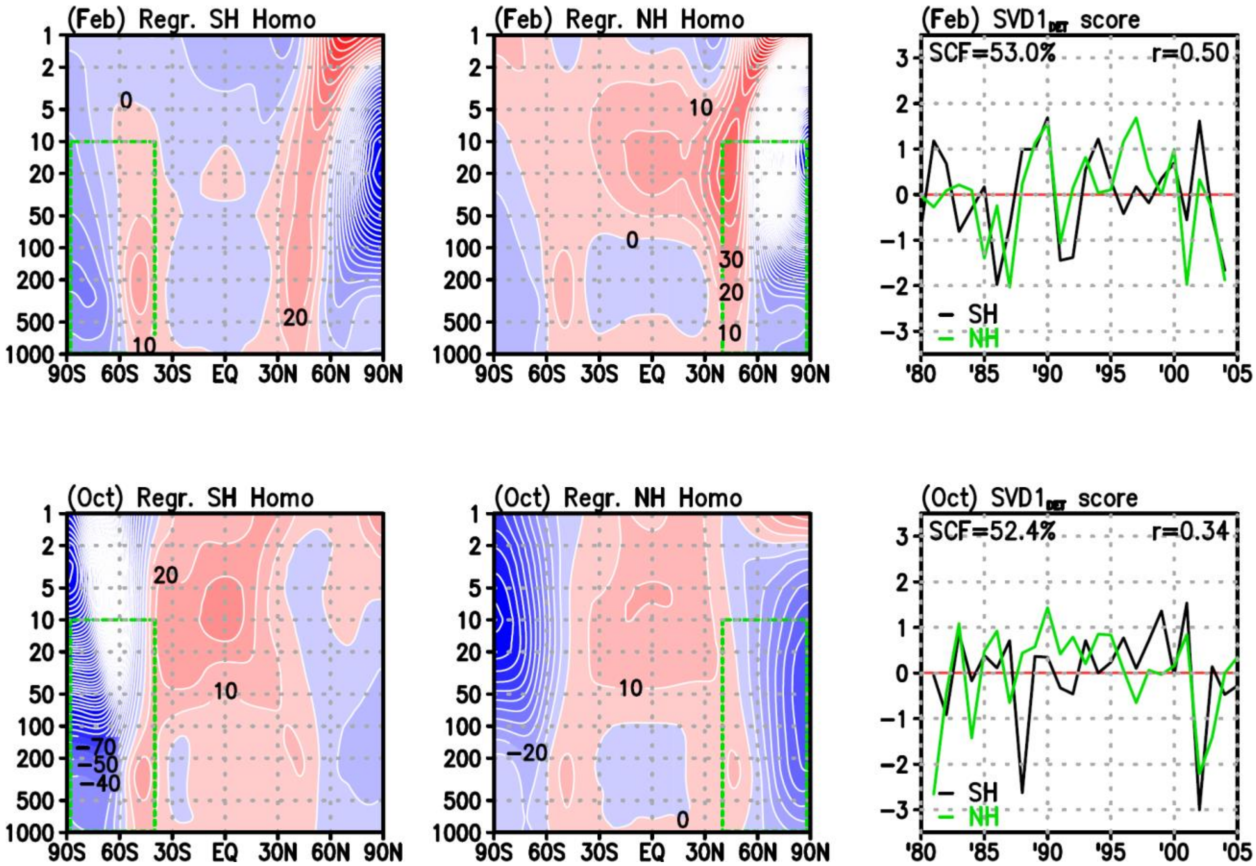

Figure 3. Zonal-mean geopotential height pattern and year-to-year variations, derived from the first SVD mode. SVD was applied to zonal-mean monthly mean geopotential heights in February (upper panels) and October (lower panels). (left column) Homogeneous regression maps for the Southern Hemisphere. Horizontal and vertical axes are latitude and altitude, respectively. (center column) Homogeneous regression maps for the Northern Hemisphere. In each month, areas within the green boxes in the Southern and Northern hemispheres were paired for the SVD calculation. The contour/color shading interval is 10 m, and red and blue colors indicate positive and negative values, respectively. (right) Time series of the normalized expansion coefficients divided by the standard deviation for the Southern Hemisphere (black curve) and the Northern Hemisphere (green curve). The squared covariance fraction (SCF) and correlation coefficient are shown in the upper left and upper right corners, respectively.

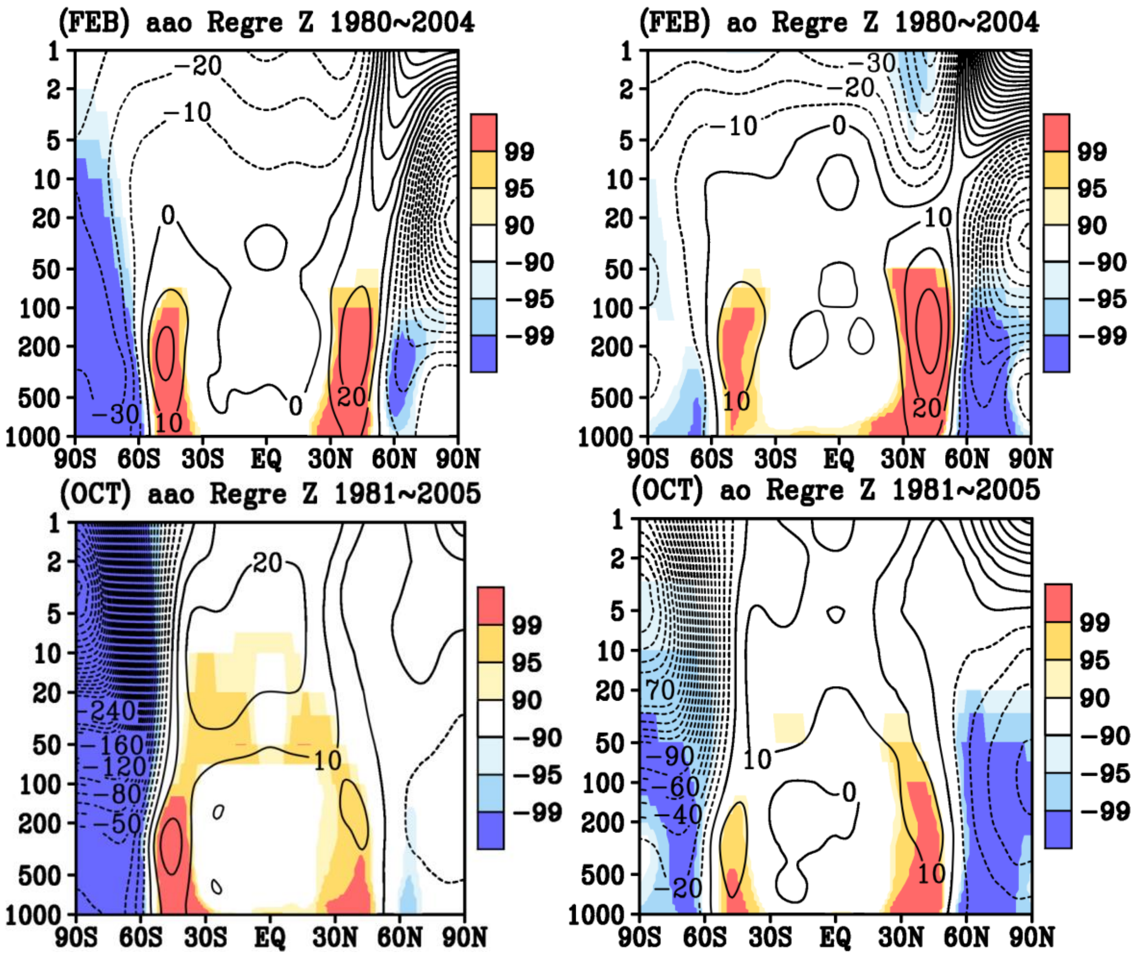

Figure 4. Meridional–vertical patterns of zonal-mean geopotential height regressed against the (left panels) AAO and (right panels) AO indices. Horizontal and vertical axes show latitude and altitude, respectively. The upper and lower panels show results for February and October, respectively. The contour interval is 10 m, and color shading indicates the level of statistical significance. Red and yellow shades indicate positive correlations, and blue shades indicate negative correlations.

Figure 1.

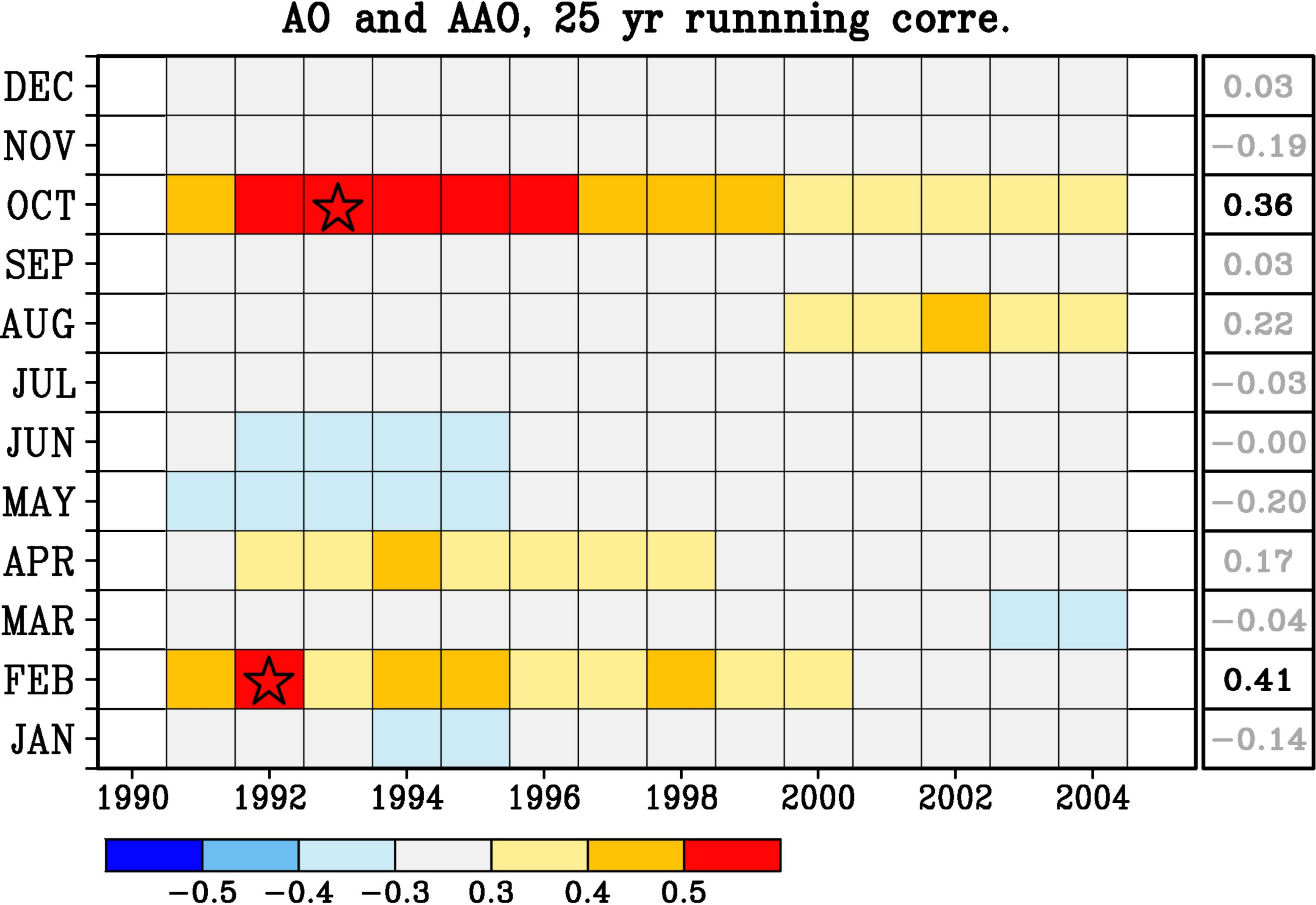
AO and AAO, 25 yr runnning corre.
DEC
NOV
OCT
SEP
AUG
JUL
JUN
MAY
APR
MAR
FEB
JAN
0.03
−0.19
0.36
0.03
0.22
−0.03
−0.00
−0.20
0.17
−0.04
0.41
−0.14
1990
1992
1994
1996
1998
2000
2002
2004
−0.5
−0.4
−0.3
0.3
0.4
0.5

Figure 2.

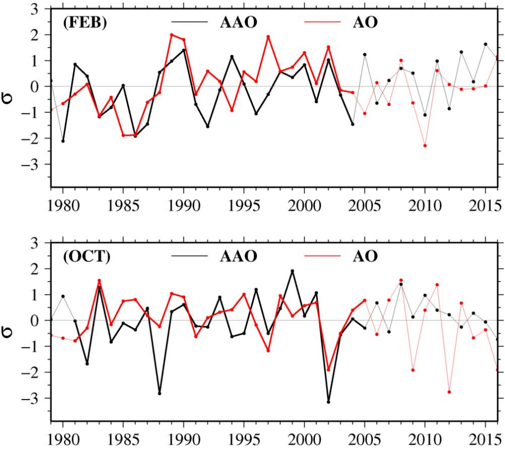
(FEB)
AAO
AO
σ
(OCT)
AAO
AO
σ
1980
1985
1990
1995
2000
2005
2010
2015

Figure 3.

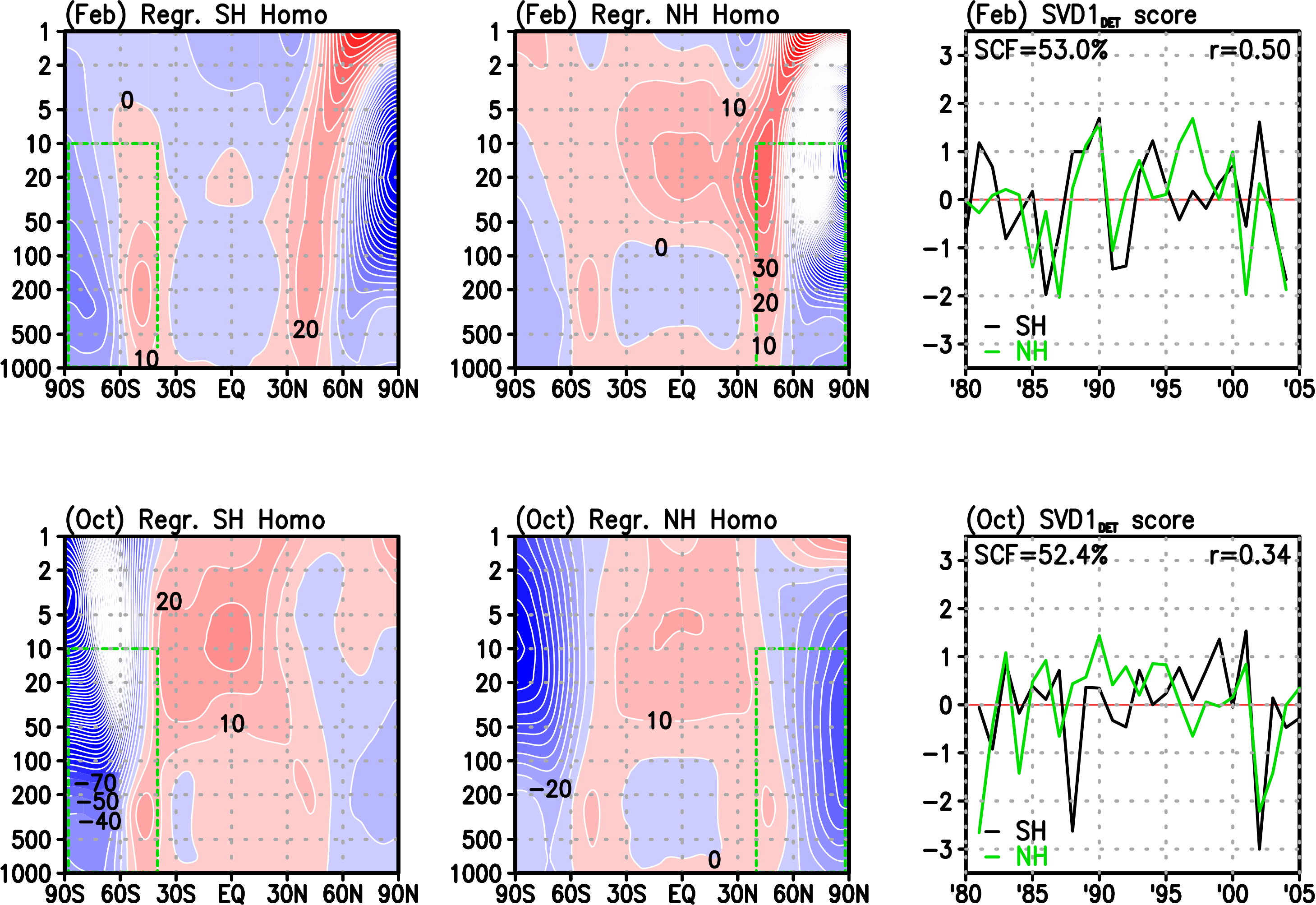
(Feb) Regr. SH Homo
(Feb) Regr. NH Homo
(Feb) SVD1DET score
SCF=53.0%
r=0.50
SH
NH
(Oct) Regr. SH Homo
(Oct) Regr. NH Homo
(Oct) SVD1DET score
SCF=52.4%
r=0.34
SH
NH
1
2
5
10
20
50
100
200
500
1000
90S 60S 30S EQ 30N 60N 90N
'80 '85 '90 '95 '00 '05
0
10
20
30
-70
-50
-40
-20

Figure 4.

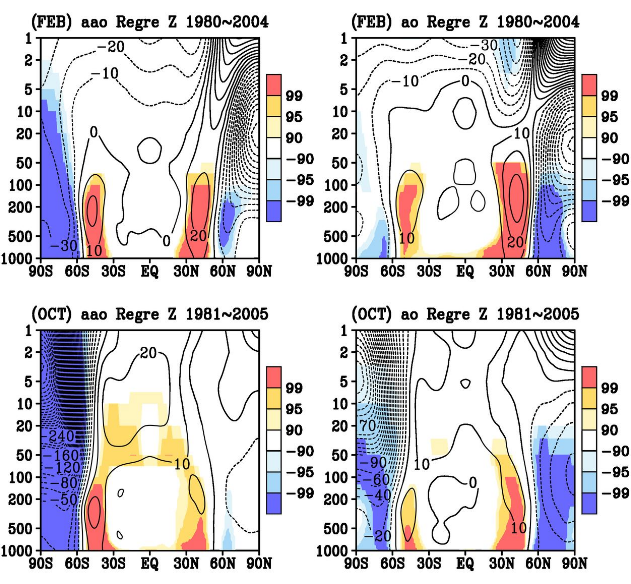
(FEB) aao Regre Z 1980~2004
(FEB) ao Regre Z 1980~2004
(OCT) aao Regre Z 1981~2005
(OCT) ao Regre Z 1981~2005
99
95
90
-90
-95
-99
90S 60S 30S EQ 30N 60N 90N
1 2 5 10 20 50 100 200 500 1000